Spectroscopy of F2 in Ne matrices

C. Bressler, W. G. Lawrence, and N. Schwentner

Citation: The Journal of Chemical Physics **105**, 1318 (1996); doi: 10.1063/1.471998
View online: http://dx.doi.org/10.1063/1.471998
View Table of Contents: http://scitation.aip.org/content/aip/journal/jcp/105/4?ver=pdfcov
Published by the AIP Publishing

Spectroscopy of F_2 in Ne matrices

C. Bressler
Institut für Experimentalphysik, Freie Universität Berlin, Arnimallee 14, D-14195 Berlin, Germany

W. G. Lawrence
Department of Chemistry, Emory University, Atlanta, Georgia 30322

N. Schwentner
Institut für Experimentalphysik; Freie Universität Berlin, Arnimallee 14, D-14195 Berlin, Germany

(Received 3 January 1996; accepted 18 April 1996)

The excited states of free and matrix-isolated F_2 were investigated in the windowless VUV region by absorption and excitation spectroscopy. In emission the $f\ ^3\Pi_g \rightarrow a\ ^3\Pi_u$ laser band of F_2 at 7.72 eV with a radiative lifetime of 2 ns and a weaker and broader band at 7.47 eV attributed to emission of F_2 aggregates are observed in an Ne matrix independent on excitation energy. The Franck–Condon envelope of the charge transfer state $C\ ^1\Sigma_u^+$ extends further to the blue by more than 1 eV in Ne (12 to 14 eV) compared to the gas phase due to a blueshift of the avoided crossing with the Rydberg $3p\pi_u(^1\Sigma_u^+)$ state. The $H\ ^1\Pi_u$ Rydberg state remains unperturbed in the Ne matrix but is blueshifted by 1.24 eV and significantly broadened due to electron–phonon coupling. A previously unreported broad absorption is observed both in the gas phase and in the matrix around 15 eV and is assigned to a strongly perturbed charge transfer state with Σ symmetry corresponding to $F^{+*}(^1S)$ and $F^-(^1S)$ ions in the dissociation limit. This charge transfer state is strongly perturbed in the gas phase by the high density of $np\pi_u(^1\Sigma_u^+)$ Rydberg states ($n \geqslant 4$) while in Ne matrix it is mixed mainly with the low-lying $4p\pi_u(^1\Sigma_u^+)$ state. The analogy of the resulting two separated groups of bands with irregular vibrational progressions to the Cl_2 case is shown. Further $np\pi_u$ and $np\sigma_u$ Rydberg progressions and the repulsive $^3\Sigma_u^+$ valence state are treated. The utility of matrix-isolated F_2 for a solid state laser is discussed. © *1996 American Institute of Physics.* [S0021-9606(96)01528-0]

I. INTRODUCTION

The bound excited electronic states of molecular fluorine are situated highest in energy among the group of halogens leading in the F_2 based VUV laser to the shortest commercially available wavelength at 157 nm (Ref. 1) from a one-photon transition. The required spectroscopy in the windowless VUV regime beyond 12 eV and the corrosiveness delayed the experimental studies of F_2 in comparison to the heavier halogens Cl_2, Br_2, and I_2. In the extensive and pioneering work of Colbourn and co-workers[2] nevertheless rotationally resolved absorption spectra of F_2 were collected in the region from 11–17 eV. They used a recording with photographic plates and the information about the intensities and the Franck–Condon envelopes of the progressions is not sufficient. It is contained in several electron-energy-loss spectra (EELS)[3–5] taken with lower resolution but the different selection rules complicate a comparison with the optical spectra. This motivated us to collect VUV absorption spectra in the gas phase (Sec. III A) with moderate resolution in order to provide spectral positions and relative intensities and to search for broad features, which are easily overlooked in the previous high-resolution measurements.

The calculations of the molecular potential surfaces culminated in the work of Cartwright and Hay,[6] in which a detailed study of the manifold of excited states and their mutual interaction was treated. They stated that the lowest optically accessible ion pair and Rydberg $^1\Sigma_u^+$ states are distorted by an avoided crossing resulting in the higher-lying $I\ ^1\Sigma_u^+(3p\pi_u)$ state. The anomalous line shape with a dramatic cut off in intensity on the blue side of the C band progression seen in the EEL spectra can be attributed to this mixing as well. A quantitative discussion of this mixing is difficult due to the limited accuracy in the calculated absolute energies of the Rydberg states which are situated at the dissociation limit 1 eV higher in energy compared to the experiment. From the large number of calculated states in the region from 11–16 eV only three of the optically accessible states, namely the C and $I\ ^1\Sigma_u^+$ and $H\ ^1\Pi_u^+$ states, have been identified in experimental spectra besides several other less well-characterized transitions.[2]

The interaction of the excited states with the host matrix has been studied in detail for NO in rare gas matrices.[7] In the gas phase, the $A\ ^2\Sigma^+$ Rydberg state and the $B\ ^2\Pi$ valence state of NO are strongly interacting, and the optical spectra are perturbed by the Rydberg-valence state mixing, while they are deperturbed to a large extent for NO in rare gas matrices.[8] Continued studies have shown that the Rydberg states are shifted to higher energies by the interaction of the extended orbital with the host matrix. The magnitude of the typical shifts of 350, 550, 850 meV and 1.2 eV in Xe, Kr, Ar, and Ne, respectively, is correlated to the size of the site of NO in the rare gas lattice. The extended electronic orbital interacts more strongly with the tight site in Ne than with the larger site in Xe. The valence transitions, on the other hand, are slightly red shifted by solvation effects and the differential shift between valence and Rydberg transition has been

 0021-9606/96/105(4)/1318/12/$10.00

used to ''experimentally deperturb'' the absorption spectrum of NO.[7]

The differential shifts are largest in Ne and this ''experimental deperturbation'' will be applied to decouple the Rydberg $3p\pi_u(^1\Sigma_u^+)$ state and the $(^1\Sigma_u^+)$ ion pair state (resulting from the intravalence $3\sigma_g \rightarrow 3\sigma_u$ transition) of F_2. As in the case of NO, the Rydberg states of F_2 will shift to higher energies while the ion pair states will be slightly red shifted due to solvation of the ion pair dipole by the host Ne matrix and an extended regular absorption of the $C\,^1\Sigma_u^+$ state is expected. A similar crossing between Rydberg and ion pair state potentials occurs in Cl_2 giving rise to a strong perturbation in the gas phase[9] which is lifted in Ar and Ne matrices.[10,11] In Cl_2 the *ab initio* calculations[12] treated the mixed states more quantitatively and the experimental gas phase studies addressed this effect in detail.[9] Therefore we will use this additional information for the discussion of the F_2 spectra.

The spectroscopic properties of fluorine embedded in rare gas crystals are also interesting with respect to solid state laser applications. In 1989 laser action in the UV was demonstrated for fluorine-doped rare gas crystals.[13] These systems use F_2 as a precursor. Photodissociation of the molecule in the lattice produces mobile F atoms which can form with codoped rare gas atoms laser active rare gas fluoride exciplexes. High densities of exciplexes can be stored in the crystals and large gain coefficients which exceed those of the gas phase by several orders of magnitude can be achieved. Stimulated emission has been reported for the $B \rightarrow X$, $C \rightarrow A$, and $D \rightarrow X$ transitions of XeF in Ar at 411 nm 540, and 286 nm, respectively, together with the $D \rightarrow X$ transition of XeF in Kr at 302 nm and XeF in neon at 269 nm.[14–18] Furthermore we have investigated the spectroscopic properties of the $D \rightarrow X$ and $B \rightarrow X$ transitions of KrF in neon at 255 and 225 nm, the $B \rightarrow X$ transition of ArF in Ne at 198 nm (Ref. 19) as well as the Rydberg states of F atoms at 94.8 and 80.1 nm together with the charge transfer state of NeF at 96.7 nm,[20] since these systems can provide shorter wavelengths. An extension to these high energies requires more detailed knowledge of the excited states of F_2 which are investigated in this paper. Only Ne with its high lying first absorption band at 17.5 eV ($n=1$ exciton) provides a suitable matrix[21] to study the matrix-isolated states of F_2 in the 11–17 eV energy interval.

In the gas phase the $f\,^3\Pi_g \rightarrow a\,^3\Pi_u$ laser transition of F_2 at 157 nm has proven its utility and we will consider the use of matrix isolated F_2 as a laser medium. This transition is from the deeply bound ion pair well of the $f\,^3\Pi_g$ state to the weakly bound $a\,^3\Pi_u$ state which, in the gas phase, dissociates yielding free F atoms. However, in the condensed phase the surrounding rare gas cage could inhibit the dissociation of F_2 and thus the high density of laser active centers could be maintained.

II. EXPERIMENT

The experiments were carried out by means of tunable synchrotron radiation in the range of 50 to 300 nm at the 3m-NIM2 beamline at BESSY, Berlin, Germany. This beamline has three exit arms and one of them was used for gas phase absorption spectra of F_2. A gas cell was mounted inside a two-step differential pumping stage and the pressure of up to 1 mbar inside the gas cell was reduced to 10^{-9} mbar in the primary monochromator. Gas mixtures of F_2/Ne (5%) were used for recording the transmission spectra with a commercial VUV-sensitive GaAsP diode. The orifice of the gas cell served as an exit slit and determined the resolution of 0.15 and 0.075 nm for two *in situ* interchangeable gratings with 1200 and 2400 l/mm, respectively. The corresponding energy resolutions of 30 and 15 meV, respectively, exceed those of about 50 meV in the available EEL spectra.

The matrix isolation studies were performed at another exit arm. The setup for spectroscopic and photochemical studies is described elsewhere.[22] The exciting light is focused to 0.2×1 mm^2 onto the substrate which is cooled by a liquid He flow cryostat to 4 K. The primary monochromator delivers more than 10^{12} photons/s within a typical bandwidth of 0.15 nm. Samples were premixed in a passivated UHV gas line and deposited by a continuous flow onto the cooled substrate. 0.1–10 μm thick samples were prepared at a deposition rate between 1 and 40 nm/s. The luminescence was analyzed in the spectral range from 60 to 600 nm with a typical resolution of 1 nm by an evacuated Seya-type VUV monochromator (60–300 nm) and by a Czerny–Turner-type UV-vis. monochromator (200–600 nm). The fluorescence was detected using an uncoated multichannel plate (MCP) or a solar blind type photomultiplier for the Seya–Namioka monochromator and by a cooled Valvo XP2020Q photomultiplier for the UV-vis. monochromator.

The samples were grown on an LiF substrate for taking excitation and fluorescence spectra. For transmission spectra a gold bar or a GaAsP diode thermally connected to the cooling finger were used as substrates since LiF is not transparent in the interesting region from 10 to 20 eV. Passing the light through the sample onto the gold substrate and collecting the reflected light through the film with the MCP detector yields transmission spectra in double pass and allows to suppress the background of scattered and fluorescence light. Alternatively the transmission was measured by the photocurrent of a GaAsP diode which served as a substrate. The F_2 absorption follows from the ratio of spectra from doped and pure Ne samples for the same thickness.

Time-resolved measurements were taken in the single-bunch mode of BESSY which provides pulse durations of about 400 ps and an interval of 208 ns between the pulses. With the standard single photon counting technique in combination with time-to-amplitude conversion[23] we achieved an instrumental response of about 700 ps (FWHM) and a temporal resolution of about 300 *ps* for lifetime measurements.

III. RESULTS

A. Gas phase absorptions

Absorption spectra of gaseous F_2 taken with 30 meV resolution are shown in Figs. 1(a) and 2(a) in the ranges from

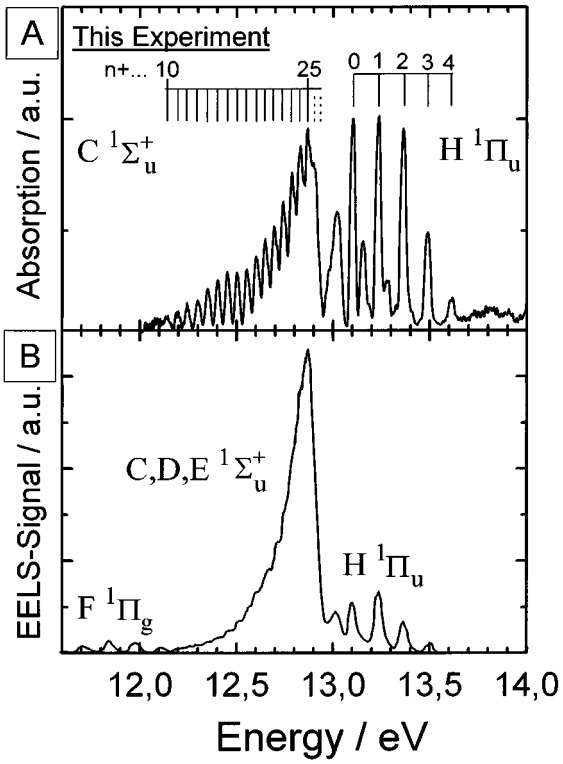

FIG. 1. Comparison of the optical absorption spectrum of F_2 in the gas phase (A) with a typical electron energy loss spectrum (EELS) (B) from Ref. 5 and the vibrational numbering of the *C* state and the *H* state (listed in Table I) is from Ref. 2 ($v'=n+26$ and 27 are only resolved in Fig. 3).

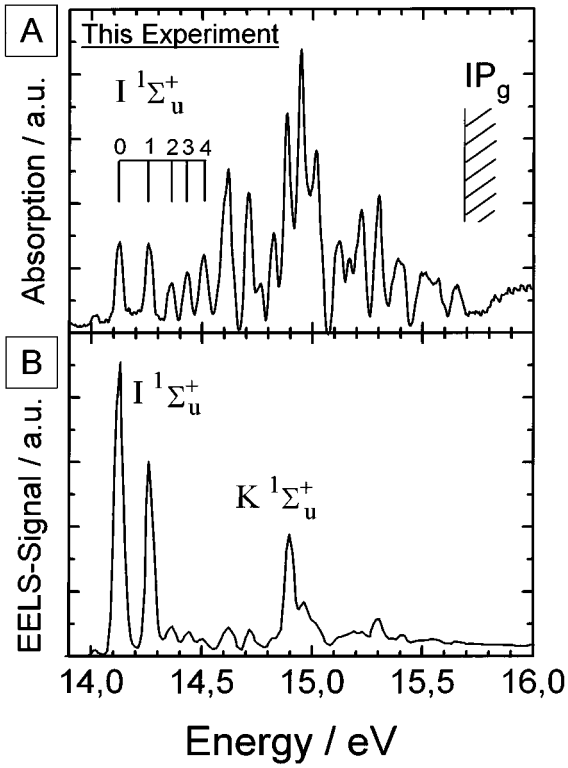

FIG. 2. Comparison of the optical absorption spectrum of F_2 in the gas phase (A) with a typical electron energy loss spectrum (EELS) from Ref. 5 (B) in the high energy region with the vibrational levels of the *I* state assigned by Ref. 2 and the first ionization potential IP_g. *K* state assignment in (B) is from Ref. 5.

12 to 14 eV and 14 to 16 eV, respectively, together with typical electron-energy-loss spectra (EELS)[5] [Figs. 1(b) and 2(b)] and with the assignments of Ref. 5.

The optically forbidden $F\ ^1\Pi_g$ state at 12 eV is only seen in the EELS at large scattering angles.[5] The vibrational levels of the $C\ ^1\Sigma_u^+$ state in the region around 12.5 eV are resolved in the optical spectrum while the EEL spectrum shows mainly the Franck–Condon envelope. Four vibrational bands of the $H\ ^1\Pi_u$ state are seen in both spectra between 13.1 and 13.5 eV and a fifth band at 13.613 eV in Fig. 1(a) can be also assigned to this progression. A significant difference in the relative strengths of the *C* and *H* bands between the optical and EEL spectra is apparent in Fig. 1. The broad band at 13.0 eV in Fig. 1 is composed of four bands according to the better resolved spectra in Fig. 3 and for the *C* state two additional vibrational members ($v'=n+26,27$) at 12.905 and 12.933 eV are also resolved in Fig. 3 close to the cut off in intensity. Three more bands (dashed ticks in Fig. 3) were attributed to the *C* state with $v'=n+28$, 29, and 30,[2] but our spectra show a strong drop in intensity right beyond $v'=n+27$, which suggests that the charge transfer state *C* terminates before the $v'=n+28$ band. The spectral positions of all the observed features are listed in Table I and compared with the previous high resolution photographic measurements of F_2 from Colbourn and co-workers.[2] A further progression with two members at 13.024 and 13.280 eV has been assigned by them as the ($v'=0$) and the ($v'=2$) members of the dipole forbidden $h\ ^3\Pi_u$ Rydberg state which is consistent with the ($v'=1$) band at 13.151 eV and the very weak ($v'=3$) band at 13.4 eV in Fig. 3 and Table I. The vibrational spacing $\omega_e \approx 1040$ cm^{-1} is typical for a Rydberg state [F_2^+, $X\ ^2\Pi$: $\omega_e \approx 1089.9$ cm^{-1} (Ref. 24)], the rotational structure with *P*, *Q*, and *R* branches[2] indicates a $\Sigma \rightarrow \Pi$ transition and the *ab initio* calculations[6] predict no further state with $^1\Pi_u$ symmetry in this region. These arguments supported the assignment to the $h\ ^3\Pi_u$ state,[2] but the rather large strength of these bands in Figs. 1(a) and 3 is in conflict with a spin forbidden $^3\Pi_u \leftarrow {}^1\Sigma_g^+$ transition in the light F_2 molecule and causes some doubts in this assignment. In addition at least three bands in the range from 12.9 to 13.2 eV [the $C\ ^1\Sigma_u^+$ ($v'=n+28$, 29 and 30) bands in Ref. 2] remain unidentified.

The situation is even more complicated in the higher energetic region shown in Fig. 2. The intensity patterns in the optical [Fig. 2(a)] and EEL [Fig. 2(b)] spectra are again quite different and an unambiguous assignment of these bands was not possible up to now. The lowest five features in Fig. 2(a) belong to states with Σ symmetry according to their rotational structure[2] and were attributed to the $I\ ^1\Sigma_u^+$ Rydberg state, although the irregular ΔG values indicate strong perturbations arising perhaps from mixing of this state with one or more nearby states of the same symmetry. In the extensive work of Colbourn *et al.* no more assignments of the states above 14.5 eV were achieved but they carefully tabulated the bands.[2] Assignments were attempted with the

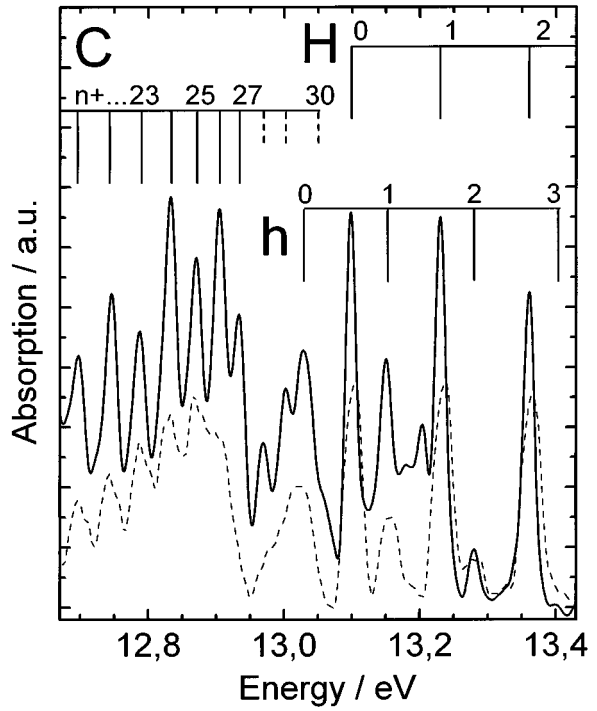

FIG. 3. Expanded region of the spectrum of Fig. 1(A) (dashed line) compared to a higher resolved spectrum (thick line) with the vibrational members of the *C*, *H*, and *h* states (listed in Table I). $v'=n+28$, 29, and 30 were assigned in Ref. 2 to members of the *C* state progression.

EELS studies of Hitchcock and co-workers,[3] but the individual bands are not sufficiently resolved in their spectrum and in the other EEL spectra[3–5] according to Fig. 2(b). They found in modeling the mixing of Rydberg transitions with charge transfer transitions a rather irregular behavior of the energy positions which strongly deviate from estimates based on quantum defects. After having reinvestigated the results of Ref. 2 they assigned more than nine perturbed Rydberg states including vibrational levels in their spectra in the 14–15.5 eV energy range. Their assignments are more tentative and discrepancies by several tenths of an eV are accepted which is unsatisfactory in view of the high density of bands evident in Fig. 2(a). The high resolution photographic plates in the energy region around 15 eV show a manifold of strongly perturbed and diffuse bands. Our spectrum contains an intense broad background in this region which we will attribute to the charge transfer $^1\Sigma_u^+$ state which dissociates into an excited $F^+*(^1S)$ and a ground state $F^-(^1S)$ ion (see Sec. IV). This broad feature can easily be lost in the photographic spectra but the relative intensities of the resolved bands riding on this background are similar in both spectra. Table II gives a compilation of the structures observed by us and in Refs. 2 and 3 together with their proposed assignments.

Only Rydberg transitions were included in the previous assignments for energies above 14 eV and due to the decrease in oscillator strength with n^{-3} for increasing main quantum number *n* a general decrease in the strength of the bands with higher energy should be expected. This expectation is not in accord with the absorption spectrum of Fig. 2(a) and especially the strongly absorbing region around 15 eV is in conflict with this assumption. The introduction of the charge transfer state mentioned above is in agreement with this experimental observation and it can explain why an assignment to Rydberg series in the past[2,3] was inconclusive. The differential shift of Rydberg and charge transfer states in a Ne matrix discussed in the introduction can help in the identification of the different contributions and matrix isolated spectra are presented next.

TABLE I. Transitions of F_2 in the gas phase in our absorption spectrum [Fig. 1(A)] compared with the values of Ref. 2. The first eight members of the *C* state have only *been* observed in emission (Emi). All entries are in eV.

This expt.	Assignments	Ref. 2
⋯	$C\ ^1\Sigma_u^+$: $v'=n+0$	11,5666(Emi)
⋯	$n+1$	11,6278(Emi)
⋯	$n+2$	11,6886(Emi)
⋯	$n+3$	11,7485(Emi)
⋯	$n+4$	11,8067(Emi)
⋯	$n+5$	11,8653(Emi)
⋯	$n+6$	11,9229(Emi)
⋯	$n+7$	11,9802(Emi)
⋯	$n+8$	⋯
⋯	$n+9$	⋯
12,139	$n+10$	12,1461
12,193	$n+11$	12,2003
12,247	$n+12$	12,2542
12,300	$n+13$	12,3069
12,352	$n+14$	12,3590
12,404	$n+15$	12,4102
12,454	$n+16$	12,4606
12,504	$n+17$	12,5109
12,553	$n+18$	12,5601
12,602	$n+19$	12,6088
12,649	$n+20$	12,6565
12,696	$n+21$	12,7032
12,742	$n+22$	12,7487
12,787	$n+23$	12,7929
12,830	$n+24$	12,8352
12,870	$n+25$	12,8740
12,905	$n+26$	12,9062
12,933	$n+27$	12,9362
12,969	$n+28$	12,9703
13,003	$n+29$	13,0057
13,029	$\mathbf{3p\sigma_u}$: $h\ ^3\Pi_u$ $(v'=0)$,	13,0182
13,04	$n+30$	13,0401
13,099	$\mathbf{3p\sigma_u}$: $H\ ^1H_u$ $(v'=0)$,	13,0936
13,151	$h\ ^3\Pi_u$ $(v'=1)$	(~13,148)
13,230	$H\ ^1\Pi_u$ $(v'=1)$	13,2261
13,280	$h\ ^3\Pi_u$ $(v'=2)$	13,2750
13,361	$H\ ^1\Pi_u$ $(v'=2)$	13,3561
13,4	$h\ ^3\Pi_u$ $(v'=3)$	⋯
13,487	$H\ ^1\Pi_u$ $(v'=3)$	13,4836
13,613	$H\ ^1\Pi_u$ $(v'=4)$	(~13,610)

B. Emission spectra and lifetimes in Ne matrix

Excitation of an F_2/Ne sample in the range of 11 to 17 eV leads to an intense emission band at 7.72 eV (FWHM=50 meV) and a weaker and broader band (FWHM ≈180 meV) at 7.47 eV (Fig. 4). The relative intensities are concentration dependent and the broad band at 7.47 eV grows with increasing F_2 concentration [Fig. 4(a)] while it

TABLE II. Our absorptions of F_2 in the gas phase (Fig. 2) compared with previous optical (Ref. 2) and electron energy loss spectra (Ref. 3) in the energy region from 14 to 16 eV together with the assignments of Ref. 2 and 3. The relative intensities of both optical spectra are also compared. All energies are in eV.

This expt.	Int.	Assignment	Ref. 2	Int.	Ref. 3	Assignment
14,125	2	$\mathbf{4p\pi_u}$: $I\ ^1\Sigma_u^+$ $(v'=0)$	14,1269		14,13	$\mathbf{4p\pi_u}$: $I\ ^1\Sigma_u^+$ $(v'=0)$
14,263	2	$I\ ^1\Sigma_u^+$ $(v'=1)$	14,2644		14,26	$I\ ^1\Sigma_u^+$ $(v'=1)$
14,360	1	$I\ ^1\Sigma_u^+$ $(v'=2)$	14,3579		14,35	$I\ ^1\Sigma_u^+$ $(v'=2)$
14,431	1	$I\ ^1\Sigma_u^+$ $(v'=3)$	14,4265		14,42	$I\ ^1\Sigma_u^+$ $(v'=3)$
			14,4404	2		
14,495	1		14,4884	3	14,48	$\mathbf{4p\sigma_u}$: $J\ ^1\Pi_u$ $(v'=0,1)$
						$I\ ^1\Sigma_u^+$ $(v'=4)$
14,522	1	$I\ ^1\Sigma_u^+$ $(v'=4)$	14,5174	1		
14,580	1		14,5685	3		
14,611	2		14,5834	3	14,60	$\mathbf{3s\sigma_g}$: $J'\ ^1\Pi_u$ $(v'=0)$
14,636	1		14,6123	4		$I\ ^1\Sigma_u^+$ $(v'=5)$
14,713	3		14,7152	4	14,70	$J'\ ^1\Pi_u$ $(v'=1)$
14,762	1					
14,826	2		14,8260	3	14,81	$J'\ ^1\Pi_u$ $(v'=2)$
14,894	5		14,8847	5	14,88	$\mathbf{5p\pi_u}$: $K\ ^1\Sigma_u^+$ $(v'=0)$
14,940	4–6					
14,959	″		14,9579	3	14,95	$K\ ^1\Sigma_u^+$ $(v'=1)$
15,006	3		15,0011	2	15,01	$K\ ^1\Sigma_u^+$ $(v'=2)$
15,037	3		15,0346	2		
15,119	3		15,1185	2	15,11	$\mathbf{5p\sigma_u}$: $L\ ^1\Pi_u$ $(v'=0)$
15,156	2		15,1723	3		
15,181	2		15,2193	3	15,21	$\mathbf{6p\pi_u}$: $M\ ^1\Sigma_u^+$ $(v'=0)$
15,225	3		15,2349	3		$L\ ^1\Pi_u$ $(v'=1)$
			15,2281	3		
15,293	3		15,2827	4	15,28	$\mathbf{6p\sigma_u}$: $N\ ^1\Pi_u$ $(v'=0)$
15,317	3		15,2970	3		$M\ ^1\Sigma_u^+$ $(v'=1)$
15,378	2		15,3571	2		
15,410	2		15,4019	3	15,39	$\mathbf{7p\pi_u}$: $O\ ^1\Sigma_u^+$ $(v'=0)$
						$\mathbf{7p\sigma_u}$: $P\ ^1\Pi_u$ $(v'=0)$

nearly vanishes for concentrations below 5000:1 (Ne/F_2) [Fig. 4(b)]. We assign the dominant and narrow emission to the $f\ ^3\Pi_g \rightarrow a\ ^3\Pi_u$ transition of isolated F_2 molecules which is in the gas phase the laser emission band of F_2 located at 7.90 eV (157 nm).[1] The red shift in the matrix by about 180 meV is attributed to the larger solvation energy of the dipole moment of the $f\ ^3\Pi_g$ charge transfer state which correlates to $F^+(^3P)+F^-(^1S)$[25] compared to the solvation energy of the $a\ ^3\Pi_u$ valence state. The lifetime of the narrow band has been measured in the single bunch mode (Fig. 5). After deconvolution of the decay curve with the instrument response a lifetime τ of 2.0 ± 0.3 ns is obtained. The estimated gas phase value of 3.7 ns (Ref. 26) is uncertain because several electronic transitions are superimposed in the same region and emission from the bottom of the $f\ ^3\Pi_g$ state is obtained

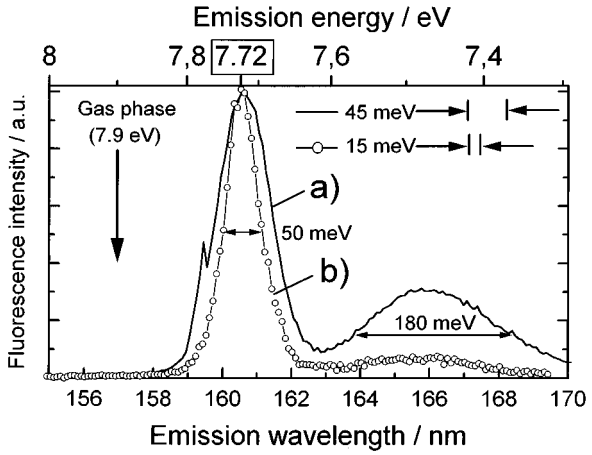

FIG. 4. Emission spectrum of the F_2 laser transition in neon matrix at two concentrations (a) 1:200 (solid line) and (b) 1:5000 (line with circles). With higher resolution (FWHM=15 meV, line with circles) the band at 7.72 has a width of 50 meV.

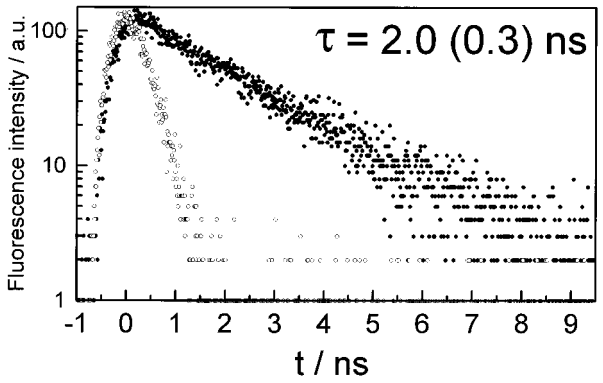

FIG. 5. Decay curve of the F_2 laser emission at 7.72 eV (full dots) together with the instrument response curve (open circles). The radiative lifetime of 2.0 ± 0.3 ns is obtained after deconvolution.

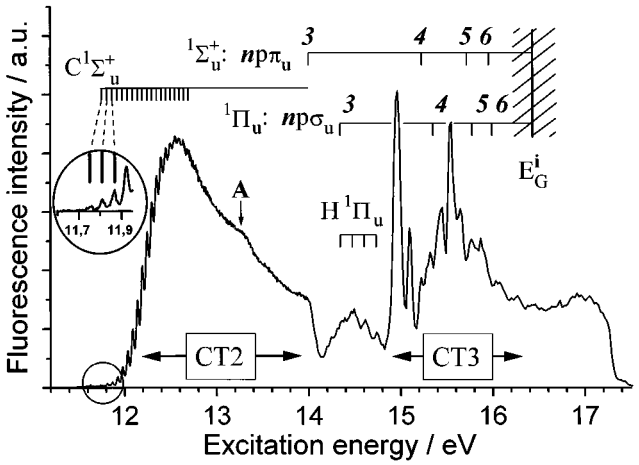

FIG. 6. Excitation spectrum of the $f\ ^3\Pi_g \rightarrow a\ ^3\Pi_u$ emission of an F_2 doped Ne matrix. The insert on the left-hand side shows the onset enlargened. The *C* state vibrational members are assigned (listed in Table II) and the calculated excitation energies for the unperturbed $np\pi_u$ and $np\sigma_u$ Rydberg series (see Table V) are shown with the hatched ionization potential in the matrix (see text). The CT2 and CT3 arrows denote the energy region of the two charge transfer states corresponding to the $F^{+*}(^1D)$–$F^-(^1S)$ and $F^{+*}(^1S)$–$F^-(^1S)$ asymptotes.

TABLE III. Comparison of transition energies of the C state in the gas phase and in neon matrix (in eV) together with the vibrational spacings $\Delta G_{v'} = G_{v'+1} - G_{v'}$ (in meV).

	Gas phase		Ne matrix	
$v' = n^+$	Transition energy	$G_{v'+1} - G_{v'}$	Transition energy	$G_{v'+1} - G_{v'}$
10	12,139	53,9	11,754	57,0
11	12,193	53,4	11,811	56,3
12	12,247	53,2	11,867	56,3
13	12,300	52,4	11,924	55,7
14	12,352	51,5	11,979	54,6
15	12,404	50,1	12,034	54,2
16	12,454	49,8	12,088	54,2
17	12,504	49,7	12,142	53,3
18	12,553	48,7	12,195	52,4
19	12,602	47,2	12,248	51,6
20	12,649	46,9	12,299	51,0
21	12,696	46,2	12,350	50,5
22	12,742	44,5	12,401	50,3
23	12,787	42,8	12,451	49,8
24	12,830	40,0	12,501	48,9
25	12,870	35,6	12,550	48,2
26	12,905	27,5	12,598	47,5
27	12,933		12,646	

with a high pressure buffer gas in order to relax the vibrational energy, which may induce a lifetime shortening. Correcting the matrix measurement of 2.0 ns for the environmental effect by[27]

$$\tau_{\text{gas}} = \tau_{\text{mat}} \left(\frac{n+2}{3} \right)^2 \cdot n, \tag{1}$$

with the index of refraction n of Ne leads to a gas phase value of 2.9 ns, which is consistent with the gas phase data within the accuracy.

The concentration dependence of the relative intensities of the 7.72 and 7.47 eV emissions and the similarity of their excitation spectra suggests that the 7.47 eV band is due to aggregates of F_2 molecules in the rare gas lattice.

C. Excitation spectra

The intensity of the F_2 emission band at 7.47 eV versus excitation energy (=excitation spectrum) is shown in Fig. 6. These spectra are taken with a higher resolution of $\Delta E \cong 10$ meV and the observed bandwidths even of the most narrow features, i.e., those of the C state exceed 25 meV and are intrinsic. A comparison with the gas phase absorption leads to the following assignments, which will be discussed in more detail in Sec. IV.

The spacings in the vibrational progression on the lower energy side of the broad band extending from 11.7 to 14 eV are comparable to those of the gas phase $C\ ^1\Sigma_u^+$ ion pair state (Table III) which justifies the indicated assignment in Fig. 6. The extension on the blue side to 14 eV in the matrix compared to 13 eV in the gas phase (Fig. 1) will be explained in Sec. IV by a blue shift of the perturbing Rydberg state in the matrix. The weak hump *A* on the smoothly decaying part of the high energy side at 13.2 eV indicates a weak contribution by a further state which will be assigned to an intermolecular charge transfer state $Ne_2^+F^-$ with the matrix. In the energy region around 14.2 eV we find a progression with four members ($\omega_e \approx 1040\ \text{cm}^{-1}$) similar to the $H\ ^1\Pi_u$ state in the gas phase, but significantly broadened and blue shifted in the Ne matrix by 1.24 eV (Table IV).

The strong band at 14.964 eV and the weaker one at 15.103 eV are separated by about 1100 cm^{-1} consistent with a regular Rydberg-type vibrational spacing. But the large intensity difference and the significantly larger width of the first band (14.964 eV) cause some doubt in an assignment to a Rydberg state. The analysis of the next bands in the region from 15 to 15.4 eV is as difficult as it is in the gas phase in the same energy region. The already mentioned strongly perturbed charge transfer absorption which remains mainly unshifted in the matrix will be offered as an explanation. At still higher energies beyond the charge transfer state four excitation bands around 15.6, 15.8, 16.1, and 16.3 eV with an intensity distribution typical for a Rydberg series and perhaps even a fifth feature around 16.4 eV can be identified. In Sec. IV we will discuss the possibility of these bands originating from the two strongest Rydberg series $1\pi_g \rightarrow np\pi_u(^1\Sigma_u^+)$ and $1\pi_g \rightarrow np\sigma_u(^1\Pi_u)$ as indicated in Fig. 6. The following unresolved continuum merges into the matrix absorption of the first ($n=1$) Ne* exciton around 17.5 eV.

The intensity in an excitation spectrum contains the absorption probability and the quantum efficiency for the relaxation to and emission from the specific emitting state and excitations which are quenched nonradiatively will be lost in an excitation spectrum. Therefore we have complemented the data with absorption spectra for the whole energy region from 10 to 17.5 eV. No further features and similar intensity ratios were observed in the absorption spectra for energies above 12.5 eV and therefore only the excitation spectra with

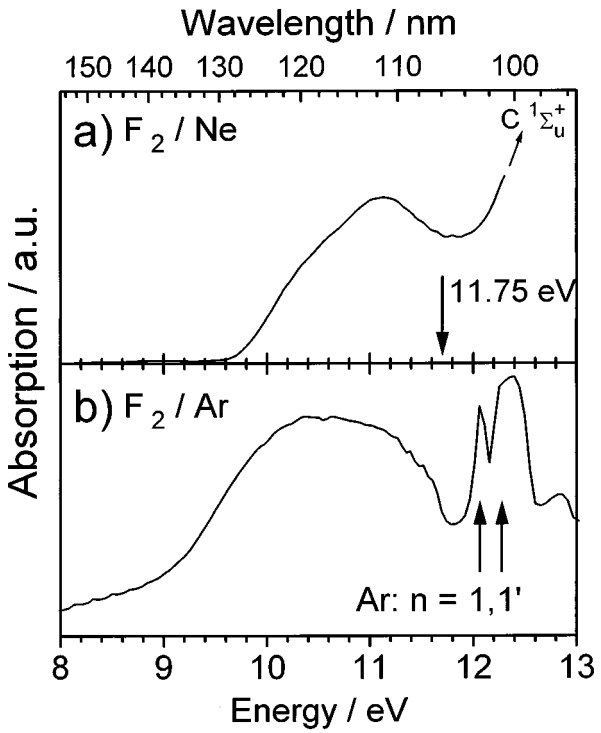

FIG. 7. Absorption spectrum of F_2 in the low energy region in Ne (a) and in Ar (b) matrices. The absorption in (a) merges into the *C* state absorption (starting at 11.75 eV) and in (b) the absorption is located just below the first Ar ($n=1, 1'$) excitonic absorptions (indicated by arrows).

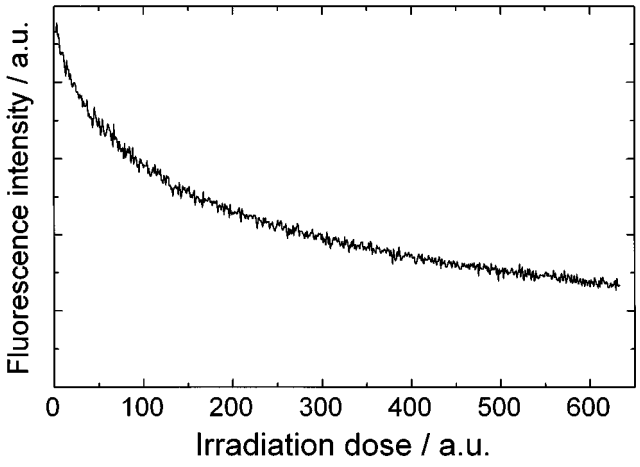

FIG. 8. Decrease of the F_2 emission intensity at 7.72 eV in a previously unirradiated Ne/F_2 sample (concentration 1:500) with 15.0 eV light due to photodissociation.

their better quality are presented. Only in the region between 10 and 13 eV an additional broad band around 11 eV showed up in the absorption spectra which is presented in Fig. 7. A similar band was found in Ar matrix around 10.6 eV. Obviously it is not a charge transfer band including a matrix atom and an assignment to a purely repulsive valence band of F_2 is proposed.

Irradiation into any of the excited states of F_2 causes a decrease of fluorescence intensity due to permanent photodissociation of the molecule (Fig. 8). The dissociation process will be considered in Sec. IV D. Simultaneously to the decrease of the F_2 laser emission band intensity we find a monotonous increase in intensity of the different atomic emission bands $F^*(3s)$ and $F^*(3s')$ and also in the $B \rightarrow X$ charge transfer fluorescence of Ne^+F^-.[20]

IV. DISCUSSION

The problems in an unambigious assignment of the absorption spectrum were already addressed and the available information is summarized in Figs. 1(a) and 3 with the identified $C\,^1\Sigma_u^+$ (dominant) charge transfer and the $H\,^1\Pi_u$ and $h\,^3\Pi_u$ Rydberg states. It was long assumed that the Rydberg state perturbing the *C* state is the $1\pi_g \rightarrow 3p\pi_u$ excitation (designated as the $G\,^1\Sigma_u^+$ state in Ref. 2), and that this state was too perturbed to be observed in the spectra. Later Cartwright and Hay[6] assumed that the higher lying *I* state (Fig. 2) just originates from the strong valence-Rydberg mixing with a large interaction matrix element of the order of 600 meV which was estimated from the separation in energy of both absorptions. Accepting their argument means that the anomalous quantum defect[2] necessary to reproduce the *I* state energy is not surprising since the unperturbed *I* state would correspond to a Rydberg state located in the region where the *C* state drops sharply in intensity and not where the perturbed Rydberg state is observed.

Since all excited states of F_2 show strong anomalies, except the $H\,^1\Pi_u$ state being due to a $1\pi_g \rightarrow 3p\sigma_u$ Rydberg excitation, it was soon recognized that mixing of the intravalence $3\sigma_g \rightarrow 3\sigma_u$ transition with the Rydberg series $1\pi_g \rightarrow np\pi_u$ can cause these severe mixing effects for the $^1\Sigma_u^+$ states and thus alter their vertical excitation energies as well as their oscillator strengths significantly.[3] A similar argument holds for the $^1\Pi_u$ states where the $1\pi_g \rightarrow np\sigma_u$ series mixes accordingly with the moderately strong $1\pi_g \rightarrow ns\sigma_u$ series[3] resulting in double well potential surfaces for each major configuration. This configuration mixing has been thoroughly examined in the calculations of Peyerimhoff and Buenker on Cl_2,[12] and the spectra of Cl_2 were explained with their potential energy diagrams. The calculations performed in Ref. 3 and 6 on F_2 show similar qualitative aspects but their limited absolute accuracy in energy does not allow an unambigous assignment of the spectra.

The shift in the cut off of the *C* state absorption spectrum in Ne (Fig. 6) illustrates that the attempt of a partial deperturbation was indeed successfull. In the following we try to derive a more complete description of the F_2 states from the additional information from the matrix spectra.

A. The $H\,^1\Pi_u$ state and the perturbation of the $C\,^1\Sigma_u^+$ state

To correlate the gas phase and matrix spectra it is necessary to determine the energy of the matrix shifted Rydberg states with respect to the ion-pair states. The $H\,^1\Pi_u$ Rydberg state is most suited for this purpose because it is not mixed with the close lying *C* state due to its different symmetry and it thus represents the only unperturbed, strong and well-

TABLE IV. Comparison of transition energies of the $3p\sigma_u(H)$ state in the gas phase and in neon matrix (in eV) together with their vibrational spacings $\Delta G_{v'}=G_{v'+1}-G_{v'}$ (in meV).

	Gas phase		Ne matrix	
State	Transition energy	$G_{v'+1}-G_{v'}$	Transition energy	$G_{v'+1}-G_{v'}$
$3p\sigma_u$	13,099	131,3	14,343	131,4
$(H\,^1\Pi_u)$	13,230	130,3	14,474	131,1
	13,361	126,3	14,605	128,0
	13,487	126,1	14,733	
	13,613		⋯	

characterized Rydberg state in the gas phase absorption spectrum (Fig. 1) corresponding to the $n=3$ member of the $np\sigma_u$ series (Fig. 6). The matrix shift in Ne amounts for Rydberg states of F atoms to 0.75 eV,[20] of Cl_2 to about 1 eV[10] and of NO to 1.3 eV (Ref. 7) together with a significant broadening of these bands. From this experience we expect for the H state a strongly broadened progression of 4 to 5 vibrational members with an onset shifted from the gas phase value of 13.1 eV to a value between 13.9 and 14.4 eV. Thus the assignment of the broad band in Fig. 6 between 14.2 and 14.8 eV with a hardly resolved vibrational structure to the $H\,^1\Pi_u$ state as indicated in Fig. 6 is obvious. The vibrational spacing of about 130 meV agrees also with that of the H state in the gas phase (Table IV) and the estimated widths in the matrix of about 120 meV is in accord with those observed for NO and F Rydberg states. The H state excitation should overlap with the weaker h state excitation when assuming the same matrix shift for both potentials, but the large widths of the vibrational states in the matrix do not allow to resolve any additional structure. The position of H $(v'=0)$ is located in the matrix at 14.343 eV when we assume similar Franck–Condon factors for the H state in the gas phase and in the matrix leading to a gas to matrix shift of 1.24 eV (Table IV). The correlation of the spectra and of the potential surfaces within the Franck–Condon region of the ground state for the $H\,^1\Pi_u$ state are displayed in Fig. 9.

The lowest vibrational level of the ionic $C\,^1\Sigma_u^+$ state observed in the gas phase absorption is located at 12.139 eV (Fig. 1 and Table III), but it is certainly not $v'=0$ since the Franck–Condon region of the ground state covers only the inner well of the C state potential (Fig. 9). The ΔG values of the 18 observed vibrational levels are shown in Fig. 10 together with literature values and with lower vibrational quanta derived from emission spectra. The uncertainty with respect to the $C\,^1\Sigma_u^+(v'=0)\leftarrow X\,^1\Sigma_g^+(v''=0)$ transition is indicated by the unknown integer n added to v' according to the nomenclature in Ref. 2. The vibrational levels in the absorption spectrum in the Ne matrix (Fig. 6) are observed at lower energies compared to the gas phase and start from 11.754 eV (Table III). We attribute this red shift in the matrix of 380 meV to a lowering of the C state potential surface by this amount (Fig. 9) due to the solvation energy of the dipole moment of this charge transfer state,[28] which is quite large for Ne with its low polarizability. The alternatives of an

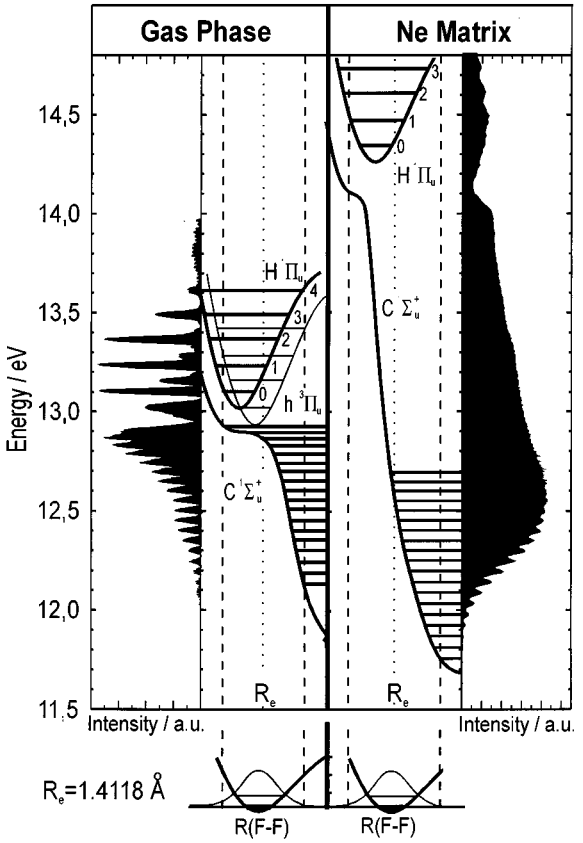

FIG. 9. Potential energy curves of F_2 in the gas phase (estimates according to Ref. 6) and in Ne matrix in the Franck–Condon region (dashed lines) of the ground state (the $X(v''=0)$ wave function is shown at the bottom). The corresponding spectra in the gas phase and in Ne matrix are plotted for comparison.

increased bond length in the ground state or a flatter inner well are less plausible. This assignment of the first observed level to $v'=n+10$ results in an increased ΔG value for the vibrational quanta in Ne (Fig. 10). Usually ΔG decreases in a matrix,[29] but an increased spacing was observed for the Schuman–Runge bands of O_2 in Ar and explained mainly by a steepening of the outer potential well.[30] The outer well of

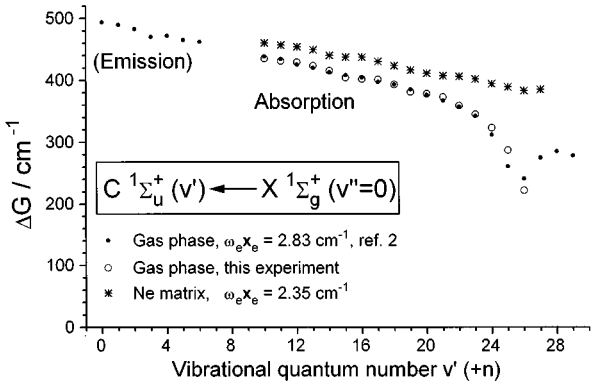

FIG. 10. Birge–Sponor plot of $\Delta G_{v'}=G_{v'+1}-G_{v'}$ vs the vibrational quantum number of the C state in the gas phase and in Ne matrix. The $v'=0$ level is not determined, and a common integer of n is added in both environments.

the C state is much shallower compared to the Rydberg states due to its ionic nature and a steepening in the tight Ne cage especially for the large elongations in the higher vibrational levels would not be surprising.

The anharmonicities in the gas phase and in matrix are quite similar in going from $v'=n+10$ to $v'=n+20$ and most interesting in our context is the behavior at even higher vibrational quanta. In the gas phase the avoided crossing with a Rydberg state (resulting from the $1\pi_g \rightarrow 3p\pi_u$ transition) of $^1\Sigma_u^+$ symmetry bends the inner well around 12.9 eV to shorter R values (Fig. 9) and as a consequence the anharmonicity increases extensively within a few quanta, and beyond $v'=n+27$ (at 12.933 eV) the spectrum breaks off (Figs. 1 and 3). The spacings of $v'=n+28,29,30$ do not fit in this trend which supports our conclusion from the intensity distribution in Fig. 3 that they do not belong to this series. In the matrix the anharmonicity of the C state levels is constant up to the highest resolved vibrational level $v'=n+28$ and the Franck–Condon envelope extends further smoothly and continuously by more than 1 eV up to 14 eV (Fig. 6) indicating the unperturbed charge transfer character in this range. Assuming the same blue shift for the perturbing Rydberg state as for the H-Rydberg state would also shift the avoided crossing by about 1.2 eV just to the observed break off in intensity in the matrix at 14 eV. The summary in Fig. 9 illustrates the remarkable changes in the spectra and in the potential surfaces due to this partial deperturbation of the C state.

In this context we come in passing to the weak feature ''A'' at 13.2 eV (Fig. 6). Since there are no other allowed F_2 transitions in this energy region we attribute it to a $Ne^+F_2^-$ exciplex. Its transition energy can be estimated by

$$E = E_G(\mathrm{Ne}) + EA^v(\mathrm{F_2}) + V(R_e), \tag{2}$$

with E_G being the ionization potential of Ne in the matrix, $EA^v(F_2)$ the vertical electron affinity of molecular fluorine and $V(R_e)$ the Coulomb interaction between the Ne^+ and F_2^- at the distance R_e of the bound ground state. The resulting value of about 13 eV supports this assignment. Since we have seen no emission which could be due to radiative relaxation of this exciplex, it shows up only after energy transfer to a nearby-lying ground state F_2 or a structural change of $Ne^+F_2^-$ resulting in an excited F_2^* which leads in both cases to the F_2 laser emission band. We prefer the first possibility since this excitation feature appeared only at higher F_2 concentrations.

Finally we consider the weak absorption observed around 11 eV which is lower in energy than the onset of the C state excitation (Fig. 7). The lack of vibrational structure as well as the absence of any fluorescence from this excitation suggests that this state is a repulsive valence state. All repulsive valence states of F_2 are dipole forbidden and an assignment to one of them is in accord with the weak measured absorption. According to Ref. 6 there are three candidates with a vertical excitation energy (in the gas phase) above 10 eV with $^{1,3}\Sigma_u^-$ and $^3\Sigma_u^+$ symmetry. The $^3\Sigma_u^+$ state is located highest in energy at 10.76 eV above the minimum of the ground state. For Cl_2 in rare gas matrices a similar broad structureless absorption just below the onset of the strong $1\,^1\Sigma_u^+$ state has been assigned to a $^3\Sigma_u^+ \leftarrow X\,^1\Sigma_g^+$ transition. In analogy we assigned the absorption around 11 eV for F_2 in Ne also to a $^3\Sigma_u^+ \leftarrow X\,^1\Sigma_g^+$ transition. The solvation of the $C\,^1\Sigma_u^+$ state in Ne matrix can lead to an increased transition probability relative to the gas phase for this spin-forbidden transition due to an intensity borrowing of this triplet state from the nearby lying singlet C state according to the calculation in Ref. 31 for the similar case of Cl_2. Therefore it is likely that this transition has not yet been observed in the gas phase.

B. A high energetic ion pair state around 15 eV

Ab initio calculations[6,25] predict three charge transfer states corresponding to $F^-(^1S)$ combined with $F^+(^3P)$, $F^+(^1D)$ and $F^+(^1S)$ at the dissociation limit. The lowest is the $f\,^3\Pi_u$ upper laser level (which cannot be seen in excitation due to the selection rules) and the second one corresponds to the charge transfer part of the perturbed $C\,^1\Sigma_u^+$ state. According to the calculations the second ion pair state leads to another potential surface with $^1\Pi_u$ symmetry and which would show up instead of the $H\,^1\Pi_u$ Rydberg state. But all these potential surfaces have double minima, one of which, at smaller internuclear distances, is Rydberg-like and one, at larger separations around 2 Å, is charge transfer like in the case of Cl_2.[12] The change of character occurs in (or near) the Franck–Condon region of the ground state. The C state has mainly charge transfer character up to the cut off region (where it changes its character) and the H state appears in absorption as a pure Rydberg state (but changing its nature towards an ion pair state at larger distances outside the FC region).

We are still left with the third ion-pair potential with only $^1\Sigma_u^+$ symmetry corresponding to the excited $F^+*(^1S)$ and $F^-(^1S)$ ions. Its energy is located about 3 eV above the charge transfer dissociation limit of the C state decaying into $F^+*(^1D)$ and $F^-(^1S)$ ions. The absorption maximum of this third ion pair state is expected around 15.5 eV, if we assume the same energy difference in the Franck–Condon region. The oscillator strength should be large[3] and due to the Rydberg-valence interaction in this range we would expect a strong mixing with the Rydberg progressions of the $np\pi_u$ series leading to irregular features in absorption. The corresponding charge transfer like absorptions should appear essentially in the same energy range in the gas phase and in the matrix, because only a weak red shift due to dipole solvation like for the C state should occur. The concentration of a high accumulated oscillator strength in the range from 15 to 16 eV in the matrix (Fig. 6) and in the gas phase (Fig. 2) is a strong indication that it originates from this third ion pair state (denoted CT3 in Fig. 6). The rather eratic intensity distribution is consistent with the expected mixing and the integrated oscillator strength is comparable to that of the C state and in marked contrast to the expected n^{-3} decay for Rydberg series. The strong bands at 14.96 and 15.10 eV in the matrix (Fig. 6) can be the inner Rydberg-type well of this perturbed potential while the broad intense background

which extends from 15.1 eV to the matrix absorption band at 16.9 eV might originate from the charge transfer part of CT3 showing an envelope comparable to that of the C state (CT2). In the next Sec. IV C we will attribute the discrete excitation features in this energy region mainly to mixing of the charge transfer $^1\Sigma_u^+$ state CT3 with the $n=4$ member of the $(^1\Sigma_u^+)$ $np\pi_u$ series. The pattern in the intensity distribution in the gas phase (Fig. 2) is different because the Rydberg progressions are situated at lower energies and it seems to be even more irregular than in the matrix. In the gas phase the I state has been assigned in Ref. 2 to the $n=4$ member of the $(^1\Sigma_u^+)$ $np\pi_u$ series with an anomalous quantum defect of $\delta=1.056$. We would rather support the interpretation in Ref. 6 which attributes this state to the $n=3$ member strongly mixed with the higher energy part of the $(^1\Sigma_u^+)$ CT2 state (the unobserved G state in Ref. 2). In both cases we would expect a strong perturbation of the line shapes as well as of the envelope of this vibrational progression. The higher lying Rydberg states in the gas phase cannot be grouped into progressions. In the gas phase they seem to coincide with the maximum of the third charge transfer state with an extremely strong perturbation. In the matrix they are shifted to higher energies beyond this maximum and the perturbation might be weakened. Therefore an identification of the Rydberg progressions in terms of quantum defects will be restricted in the next section to the matrix case.

Finally we mention that we also considered to correlate the $I\ ^1\Sigma_u^+(v'=0,1)$ bands in Fig. 2 (gas phase) with the two bands at 14.96 and 15.10 eV in Fig. 6 (matrix) and thus blue shifted by 0.8 eV due to their Rydberg character. This seems to be too simple because the widths and the intensity distributions in the whole v' progression are not consistent. The interaction with a strong charge transfer state has to be included anyway and a more involved interpretation concerning the different perturbations in the matrix and in the gas phase by the ion pair states is necessary.

C. Ionization potential and the $1\pi_g \rightarrow np\pi_u(^1\Sigma_u^+)$ and $1\pi_g \rightarrow np\sigma_u(^1\Pi_u)$ Rydberg series

In Sec. IV A we identified the rather unperturbed $H\ ^1\Pi_u$ Rydberg state in the matrix which is the $n=3$ member of the $n\pi\sigma_u$ series. For F atoms in Ne it was shown that the gas phase quantum defects are well suited to describe several Rydberg series[20] which is an interesting observation in view of the revived discussion of the quantum defect and effective mass approximation concepts.[32] Keeping therefore the gas phase $H\ ^1\Pi_u$ quantum defect $\delta_{\text{gas}}=0.707$ constant in the matrix corresponds to a shift of the first ionization potential by the H state matrix shift of 1.24 eV from $IP_g=15.686$ eV (Ref. 33) to $E_g^i=16.930$ eV. The vertical matrix and gas phase ionization energies are also connected by

$$E_g^{\mathbf{i}}=IP_g+P_+ +V_0, \tag{3}$$

where P_+ is the polarization energy of the ionic core and V_0 is the polarization energy of the electron. The sum $P_+ + V_0$ is the blue shift of the gas phase ionization energy and implies that P_+ has a value of about 2.6 eV if we take the electron affinity of Ne of -1.4 eV as determined from photoelectron spectroscopy.[34] This core solvation energy is larger than estimates in the range of 1 eV to 1.8 eV (Ref. 7) and a smaller blue shift of the ionization potential is more probable.

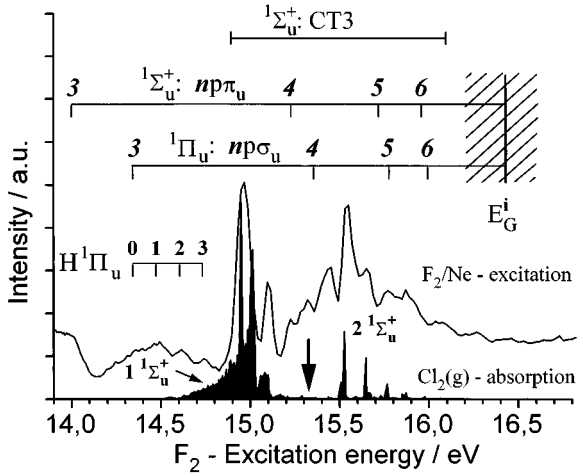

FIG. 11. Enlargened region of the F_2 excitation spectrum together with the gas phase absorption of Cl_2 shifted by about 6 eV for comparison of the absorption features with the assignments of Ref. 9 in Fig. 6. The arrow indicates the energy of the unperturbed states in Cl_2.

Therefore we have shifted the ionization potential in Ne to $E_G^i=16.44$ by 0.75 eV in Fig. 6 just as observed for F atoms in Ne.[19] The hatched area around E_G^i indicates the uncertainty for this matrix shift, and the chosen value seems to be more realistic in view of the arguments given above. In this case the quantum defect δ necessary to reproduce the $H(v'=0)$ energy has to be reduced from $\delta_{\text{gas}}(np\sigma_u)=0.707$ (Ref. 2) to $\delta_{\text{mat}}(np\sigma_u)=0.450$. Similarly the energy of the diabatic $3p\pi_u$ Rydberg state (estimated near 14 eV) is reduced from $\delta_{\text{gas}}(np\pi_u)=0.866$ (Ref. 2) to $\delta_{\text{mat}}(np\pi_u)=0.637$. Since there exists no unperturbed Rydberg state with $^1\Sigma_u^+$ symmetry this quantum defect is more tentative. The predicted $(v'=0)$ band of each member in the two series using the δ_{mat} values would be located at the positions marked in Fig. 6 with an uncertainty of 0.5 eV if the uncertainty of the matrix ionization potential is included.

The $n=4$ member of the $(^1\Sigma_u^+)np\pi_u$ series is thus located at 15.3 eV. Introducing now the interaction of this diabatic Rydberg state with the $(^1\Sigma_u^+)$ charge transfer potential (CT3 in Fig. 6) leads to new, adiabatic potential surfaces which can explain the irregular shape of the excitation spectrum in the region from 14.8 to 16 eV according to the following arguments.

An expanded view of the F_2 excitation spectrum with the $np\pi_u$ and $np\sigma_u$ series and CT3 is compared in Fig. 11 with the absorption spectrum of Cl_2 in the region of the $1\ ^1\Sigma_u^+$ and $2\ ^1\Sigma_u^+$ transitions. For the comparison the strongest band of the $1\ ^1\Sigma_u^+$ transition at 9.1 eV was shifted to 14.9 eV to give an impression of the similarity in the structure of the Cl_2 and F_2 spectra. This part of the Cl_2 spectrum was thoroughly examined[9] and is well understood. It originates from two adiabatic potential surfaces of valence and Rydberg type

which would cross within the Franck–Condon region inbetween the $1\,^1\Sigma_u^+$ and $2\,^1\Sigma_u^+$ absorptions at an energy which is marked by an arrow.[9] The strong interaction and mixing of the two potential surfaces causes the minimum in absorption just in the crossing region and the splitting in the $1\,^1\Sigma_u^+$ and $2\,^1\Sigma_u^+$ groups with their irregular vibrational structure. In close analogy the predicted unperturbed $4p\pi_u$ Rydberg state of F_2 and thus its crossing with the CT3 state is situated right at the arrow marking the crossing in the Cl_2 case. For a similar strong mixing of the $4p\pi_u$ state with CT3, which have the same symmetry, it is obvious to correlate the strong excitation band at 14.9 eV with the $1\,^1\Sigma_u^+$ features and the strong structures around 15.5 eV with the $2\,^1\Sigma_u^+$ features and the analogy in the size of the splitting as well as in the irregular vibrational structure is quite striking. The strong excitation band at 14.96 eV would then be the dominant charge transfer part of the mixed Rydberg $(4p\pi_u)$ valence (CT3) potential terminating at 15.0 eV and the excitation features from 15.5 to 16 eV are due to the higher lying (mixed) potential well above the avoided crossing. The weaker and narrower band at 15.10 eV could result from perturbations similar as in the Cl_2 absorption and the growing excitation intensity from 15.2 to 15.5 eV might be assigned to this configuration mixing as well. The higher members of this series should also contribute to mixing with CT3 but with a reduced intensity according to the decreasing overlap of the extended Rydberg electronic orbitals with the valence configuration of CT3. We cannot distinguish in our spectra between the higher mixed potentials and the strong contribution of the $n=4$ member. It is possible, that the absorption features around 15.8 and 16.0 eV stem from the $n=5$ and $n=6$ members of the $np\pi_u$ series mixed with CT3.

Next we consider the second Rydberg series $(^1\Pi_u)np\sigma_u$ with different symmetry. The intensity of the $3p\sigma_u$ transition (H state) is already weaker than that of the charge transfer mixed $4p\pi_u$ band. Nevertheless the $4p\sigma_u$ Rydberg state predicted at 15.356 eV $(v'=0)$ can be responsible for part of the excitation intensity especially in the range from 15.2 to 15.5 eV where a minimum is expected for the mixed $^1\Sigma_u^+$ transitions according to the discussed comparison with Cl_2. Assigning the higher energetic features around 15.7 and 16 eV to the $(^1\Pi_u)np\sigma_u$ series $(n=5,6)$ seems to be doubtful with respect to the expected stronger $(^1\Sigma_u^+)$ mixed states.

D. Photodissociation with respect to solid state laser application

Several processes can contribute to F_2 dissociation in the neon matrix upon VUV excitation. Radiative relaxation of F_2 at 160.6 nm (7.72 eV) starts from the bottom of the $f\,^3\Pi_g$ state and terminates on the weakly bound a $^3\Pi_u$ state. According to the calculations by Ref. 25 the minimum of the $f\,^3\Pi_u$ state is situated around 2 Å which lies within the bound part of the state[6] and therefore no dissociation after radiative relaxation is expected. This is in accord with our observed linewidth of 50 meV for the emission which indicates that the lower potential is flat in the FC region. The width in the matrix is even about a factor of 2 smaller than in the gas phase[1] where vibrational structure was observed in the spontaneous emission with a spacing of 312 cm^{-1}. The small width suggests that the emission in the neon matrix corresponds to the $f\,^3\Pi_g(v'=0)\rightarrow a\,^3\Pi_u(v''=0)$ transition which will indeed prevent dissociation.

Higher kinetic energies can be imparted to the F atom fragments by predissociation in the manifold of excited states consisting of singlet surfaces which are populated by photoexcitation and triplet surfaces which are populated by nonradiative relaxation. The dissociation observed in Fig. 8 originates from the kinetic energy acquired in these processes similar to the Cl_2 case.[12] Dissociation occurs for the repulsive $^3\Sigma_u^+$ state and also all bound excited states implying an efficient predissociation of all excited bound states of F_2.

The $f\,^3\Pi_g\rightarrow a\,^3\Pi_u$ gas phase laser transition is the only emission occurring in the matrix and it could be useful for a 160.6 nm solid state laser in the neon matrix. The measured lifetime is close to the estimated radiative one, indicating weak nonradiative quenching and a high quantum efficiency together with an efficient funneling into the emitting state. Solid state exciplex lasers have demonstrated high efficiency due to high density of excited states which can be achieved in these F_2 doped neon matrices. However, the use of F_2 in the neon matrix as a laser medium may be complicated by the photodissociation of F_2. Continued irradiation will deplete the F_2 concentration. Higher concentrations of F_2 may allow to build up a steady-state concentration of molecules (Fig. 8), but clustering, which changes the emission properties (Fig. 4) and perhaps reduces the quantum yield of emission, can reduce the laser efficiency.

V. CONCLUSIONS

Excitation of F_2 in a matrix of neon produces emission at 7.72 eV which is assigned to the $f\,^3\Pi_g(v'=0)\rightarrow a\,^3\Pi_u(v''=0)$ transition. A weaker, concentration dependent, emission is observed at 7.47 eV and is assigned to cluster or dimer emission. The excitation spectrum of matrix-isolated F_2 is significantly deperturbed compared to the gas phase absorption spectrum and the electron energy loss spectra. This difference is attributed to the interaction of the excited states of F_2 with the neon lattice. *Ab initio* calculations and experimental studies of both Cl_2 and F_2 show that the ion pair and Rydberg states are strongly mixed. Moreover, our spectra reveal both in the gas phase and in the Ne matrix a second unreported broad absorption belonging to the higher lying charge transfer state which correlates to the $F^{+*}(^1S)$ and $F^-(^1S)$ asymptote. We have used the *ab initio* calculations to qualitatively describe how the ion pair and Rydberg states interact with the neon matrix and how the diabatic states mix to form the adiabatic states observed in the excitation spectrum. It is shown that the ion pair states and the Rydberg states are less perturbed in the Ne matrix, because the Rydberg states interact strongly with the neon lattice and are thus shifted by more than 1 eV to higher energy. The effect of the mixing of these states is most clearly seen in the excitation of the *C* state which is composed of a strongly

mixed $^1\Sigma_u^+$ ion pair state [dissociating into $F^+*(^1D)$ and $F^-(^1S)$] and a $^1\Sigma_u^+$ Rydberg state corresponding to the $1\pi_g \rightarrow 3p\pi_u$ excitation. In addition the perturbed excitation spectrum in the matrix above 15 eV is due to a similar mixing of the $4p\pi_u$ member with the third charge transfer state expected in this energy range, while the higher members of this series and of the $1\pi_g \rightarrow np\sigma_u(^1\Pi_u, n \geq 4)$ series contribute to a minor extent. The $H\,^1\Pi_u$ state is blue shifted by 1.24 eV and broadened to about 120 meV due to electron–phonon coupling of the vibrational levels with the Ne lattice, but its regular structure is conserved in both environments. The H state is also composed of mixed Rydberg and ion pair states, however in the Franck–Condon region of the F_2 ground state, this potential is of Rydberg character.

Permanent loss of the fluorescence at 7.72 eV due to photodissociation of F_2 is observed upon continued excitation in the range above 11.75 eV. The dissociation of F_2 occurs by predissociation in the manifold of excited states. The kinetic energy imparted to the F atom fragments is thus sufficient to overcome the neon cage barriers. While molecular fluorine may be useful as a condensed phase laser medium, the photodissociation of F_2 limits the efficiency of this system.

ACKNOWLEDGMENTS

We would like to thank the group of Professor Schmoranzer (Uni Kaiserslautern) for providing us with their differential pumping stage for the gas phase absorption measurements. We are indepted to the BESSY staff, especially Dr. G. Reichardt, for their encouraging support. This work was financed by the *Bundesministerium für Forschung und Technologie* via Contract No. 055KEAYB5. W.G.L. acknowledges financial support by a DAAD and an NSF fellowship.

[1] J. R. Rice, A. K. Hays, and J. R. Woodworth, Appl. Phys. Lett. **31**, 31 (1977).
[2] E. A. Colbourn, M. Dagenais, A. E. Douglas, and J. W. Raymonda, Can. J. Phys. **54**, 1343 (1976).
[3] A. P. Hitchcock, C. E. Brion, G. R. J. Williams, and P. W. Langhoff, Chem. Phys. **66**, 435 (1982).
[4] R.-G. Wang, Z.-W. Wang, M. A. Dillon, and D. Spence, J. Chem. Phys. **80**, 3574 (1984); H. Nishimura, D. C. Cartwright, and S. Trajmar, *ibid*. **71**, 5039 (1979).
[5] K. Hoshiba, Y. Fujita, S. S. Kano, H. Takuma, T. Takayanagi, K. Wakija, and H. Suzuki, J. Phys. B L875 (1985).
[6] D. C. Cartwright and P. J. Hay, Chem. Phys. **114**, 305 (1987); see also P. J. Hay and D. C. Cartwright, Chem. Phys. Lett. **41**, 80 (1976); D. C. Cartwright and P. J. Hay, Chem. Phys. **70**, 3191 (1979).
[7] M. Chergui, N. Schwentner, and W. Böhmer, J. Chem. Phys. **85**, 2472 (1986).
[8] M. Chergui and N. Schwentner, J. Chem. Phys. **97**, 2881 (1992).
[9] J. Wörmer, T. Möller, J. Stapelfeldt, G. Zimmerer, D. Haaks, S. Kampf, L. LeCalve, and M. C. Castex, Z. Phys. D **7**, 383 (1988).
[10] P. Gürtler, H. Kunz, and J. Le Calvé, J. Chem. Phys. **91**, 6020 (1989).
[11] J. G. McCaffrey, H. Kunz, and N. Schwentner, J. Chem. Phys. **96**, 155 (1992).
[12] D. Peyerimhoff and R. J. Buenker, Chem. Phys. **57**, 279 (1981).
[13] N. Schwentner and V. A. Apkarian, Chem. Phys. Lett. **154**, 413 (1989).
[14] G. Zerza, R. Kometer, G. Sliwinski, and N. Schwentner, Proc. SPIE **1397**, 346 (1990).
[15] G. Zerza, G. Sliwinski, and N. Schwentner, Appl. Phys. A **54**, 106 (1990).
[16] G. Zerza, G. Sliwinski, and N. Schwentner, Appl. Phys. A **55**, 331 (1992).
[17] A. I. Katz, J. Feld, and V. A. Apkarian, Opt. Lett. **14**, 441 (1989).
[18] G. Zerza, G. Sliwinski, and N. Schwentner, Appl. Phys. A **56**, 156 (1993).
[19] C. Bressler, W. G. Lawrence, and N. Schwentner (unpublished).
[20] C. Bressler, W. G. Lawrence, and N. Schwentner, J. Chem. Phys. **102**, 48 (1995).
[21] N. Schwentner, E. E. Koch, and J. Jortner, in *Electronic Excitations in Condensed Rare Gases* (Springer Tracts in Modern Physics, Springer, New York 1985), Vol. 107.
[22] J. Bahrdt, P. Gürtler, and N. Schwentner, J. Chem. Phys. **86**, 6108 (1987).
[23] I. H. Munro and N. Schwentner, Nucl. Instrum. Meth. **208**, 819 (1983).
[24] R. P. Tuckett, A. R. Dale, D. M. Jaffey, P. S. Jarrett, and T. Kelly, Mol. Phys. **49**, 475 (1983).
[25] T. Sakai, K. Tanaka, A. Murakami, H. Iwaki, H. Terashima, and T. Shoda, J. Phys. B **21**, 229 (1988).
[26] M. Diegelmann, K. Hohla, F. Rebentrost, and K. L. Kompa, J. Chem. Phys. **76**, 1233 (1982).
[27] R. L. Fulton, J. Chem. Phys. **71**, 4141 (1974).
[28] D. C. McKean, Spectrochim. Acta A **23**, 2405 (1967).
[29] M. E. Jacox, J. Phys. Chem. Ref. Data **13**, 945 (1984).
[30] O. Schnepp and K. Dressler, J. Chem. Phys. **42**, 2482 (1965); E. Boursey, J.-Y. Roncin, and N. Damany, Chem. Phys. Lett. **5**, 584 (1970).
[31] F. Grein, S. D. Peyerimhoff, R. J. Buenker, Can. J. Phys. **62**, 1928 (1984).
[32] H. H. v. Grünberg and H. Gabriel, J. Chem. Phys. **103**, 6040 (1995).
[33] J. Berkowitz, W. A. Chupka, P. A. Guyon, J. H. Holloway, and R. Spohr, J. Chem. Phys. **54**, 5165 (1971).
[34] N. Schwentner, F. J. Himpsel, V. Saile, M. Skibowski, W. Steinmann, and E. E. Koch, Phys. Rev. Lett. **34**, 528 (1978).